Vol. 49 (2018) *ACTA PHYSICA POLONICA B* No 3

EVOLUTION OF γ COLLECTIVITY — (n,γ) SPECTROSCOPY OF ^{98}Mo WITH FIPPS*

J. Wiśniewski, W. Urban, T. Rząca-Urban

Faculty of Physics, University of Warsaw, Warszawa, Poland

U. Köster, C. Michelagnoli, M. Jentschel, P. Mutti

Institut Laue-Langevin, Grenoble, France

(Received January 16, 2018)

Excited states in ^{98}Mo have been populated in (n,γ) reaction and studied using γ-ray coincidences measured with Germanium Clover detectors of the new instrument FIPPS. The aim of the study is to investigate the evolution of γ collectivity in Mo isotopes in its early-development stage. The ground state of ^{97}Mo $5/2^+$ should allow the observation of the γ band in ^{98}Mo up to spin 7^+. This is sufficient to measure interesting properties of the γ band, such as mixing ratios.

DOI:10.5506/APhysPolB.49.547

The emergence of a deformation in atomic nuclei is one of the most important subjects of nuclear structure studies. The region of neutron-rich nuclei with masses $A \approx 100$ is a place where the evolution of nuclear deformation can be studied experimentally in detail. Of particular interest are the mechanisms which create nuclear deformation. In the $A \approx 100$ region two such mechanisms are recognized so far. The population of the "deformation-driving", low-Ω subshells of the $h_{11/2}$ neutron intruder orbital [1] and the particular role of the neutron $9/2^+[404]$ extruder orbital [2]. Recently, another mechanism have been proposed. Observation of the sudden onset deformation in this region at neutron number $N = 59$ may also be caused by the so-called type II shell evolution, related to the promotion of protons to the $g_{9/2}$ orbital, leading to quantum phase transition [3].

Another interesting phenomenon in this region is the evolution of gamma deformation. The gamma collectivity is probably the first collective effect that develops when valence particles are added to an inert core. It was

* Presented at the XXXV Mazurian Lakes Conference on Physics, Piaski, Poland, September 3–9, 2017.

observed at $N = 52$ and $N = 53$ in Se and Kr isotopes [4–6] and is present above the $N = 50$ shell closure in all nuclei from Ge to Ru [7]. An analogous effect was recently observed just above the $N = 82$ shell closure in the $N = 86$ Te, Xe, Ba and Ce isotones [8, 9], where it was found that γ excitations evolve from irregular in Te to more collective bands in Ba and Ce nuclei, as illustrated in Fig. 1. This evolution is accompanied by particular changes in the properties of γ-ray transitions, *e.g.* M1/E2 mixing ratios. It is of interest to study systematically this evolution, in order to describe the role of γ collectivity in the development of nuclear deformation.

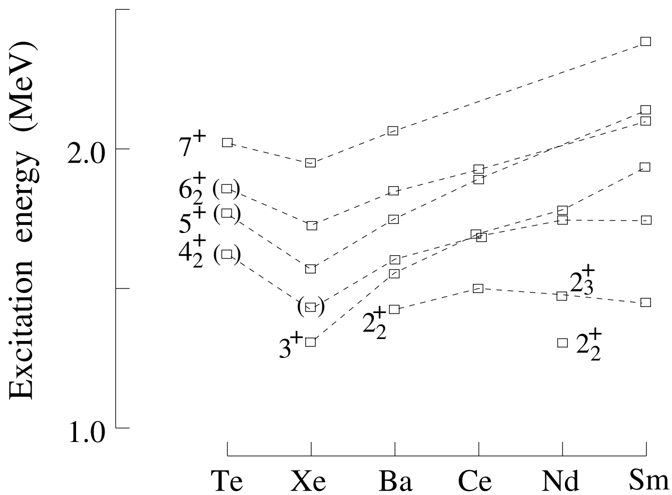

Fig. 1. Energies of positive-parity levels in $N = 86$ isotones [9].

The γ collectivity can be studied in detail in the $A \approx 100$ region, where it is well-established in Mo and Ru isotopes. In Mo isotopes, the γ degree of freedom is well-studied for neutron numbers $N > 61$ [10–12], but its emergence in lighter isotopes is less known. As suggested by the calculations [13], γ deformation appears first in ^{98}Mo and is already well-developed in ^{100}Mo. Because these nuclei are easily accessible experimentally, one could study the evolution of γ collectivity in its early development stage.

Of particular importance in such studies are precise spin-parity assignments to excited levels in nuclei. A new instrument FIPPS dedicated for precision measurements of nuclei produced in neutron-capture reactions has been constructed at ILL Grenoble, as a successor of the EXILL setup. The FIPPS array is ideally suited for precise and detailed studies of transition multipolarities. High symmetry of the FIPPS array, based on the octagon geometry, provides 3-angles for angular-correlation measurements, while the use of Clover Ge detectors in the array, which serve as Compton polarimeters, enables linear-polarization measurements.

In this paper, we present some preliminary results from our recent measurement on ^{98}Mo performed with FIPPS. The ^{98}Mo nuclei were produced in thermal-neutron capture on a ^{97}Mo target. The spin-parity of the ground state of ^{97}Mo, $5/2^+$, should allow the observation of the γ band in ^{98}Mo up to spin 7^+. This is sufficient to measure interesting properties of the γ band, such as mixing ratios.

High efficiency of FIPPS provided a very high rate of coincidence events, resulting in collecting 1.5×10^{10} triple-γ events, allowing the unique construction of a detailed excitation scheme of ^{98}Mo. From the analysis, a significantly extended scheme is expected. As an example, in Fig. 2 we show a γ-ray spectrum doubly-gated on the 5680.0-keV primary transition and on the 787.4-keV ground-state transition. In the spectrum, one observes peaks corresponding to transitions linking the 2962.3- and 787.4-keV levels. In addition to the known 945.0- and 1452.5-keV transitions depopulating the 2962.4 keV level, there are three new decays from this level with energies of 738.7, 1204.3 and 2175.1 keV. In Fig. 3, we present the relevant part of the excitation scheme.

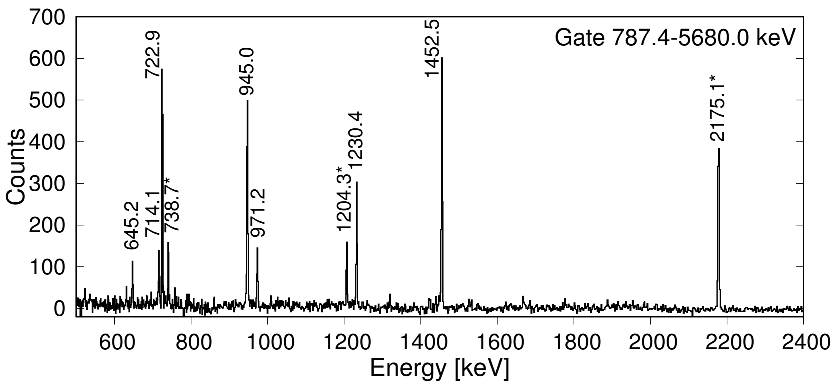

Fig. 2. A γ-ray spectrum doubly-gated on 787.4 and 5680.0 keV lines. Energies are given in keV. New lines are marked with asterisks.

High-quality detectors of FIPPS enabled precise energy calibration up to 8 MeV, based on ^{28}Al lines. Second order polynomial was fitted to experimental data with $\chi^2/N = 0.75$. Figure 4 (a) shows deviations from the fit for several ^{28}Al lines, illustrating the precision of the calibration. We expect that using the calibration will provide an order-of-magnitude more precise neutron-binding energy for ^{98}Mo than the present value. Figure 4 (b) shows details of the gain-matching procedures of the data, illustrating the precision of line tracking when recalibrating detector to a common calibration.

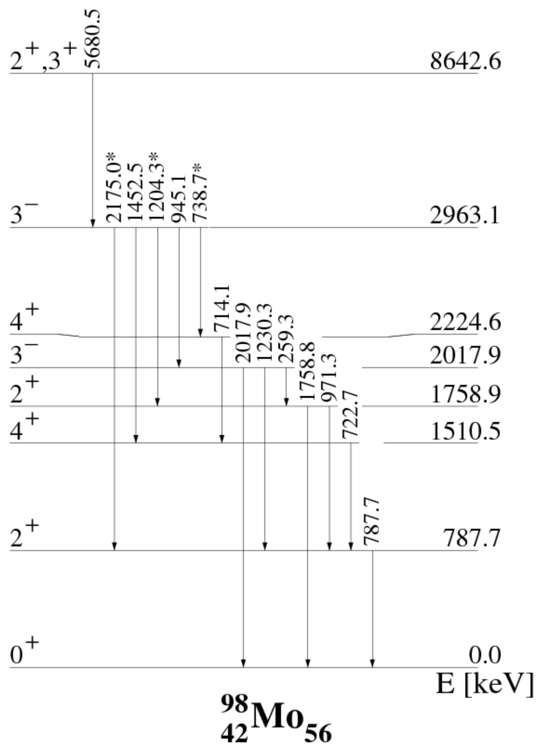

Fig. 3. Partial scheme of excited states in ^{98}Mo, populated in (n, γ) reaction discussed in the present work. New lines are marked with asterisks.

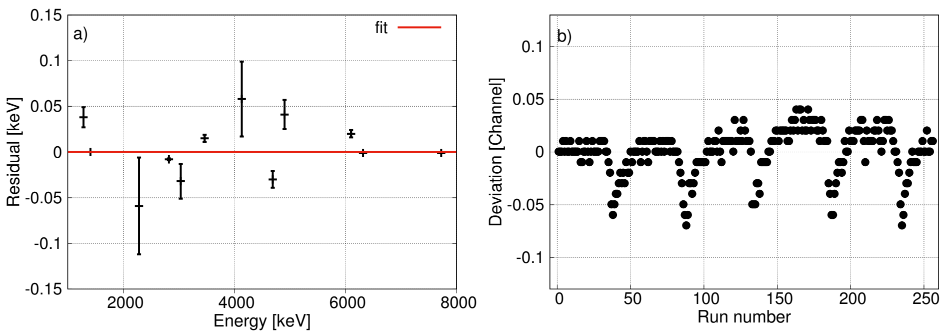

Fig. 4. (a) Deviations of the calibration data from the fitted energy calibration. (b) Position of the 787.4 keV level in ^{98}Mo: each point represents a 10-minutes run.

While the analysis of angular correlations and directional-polarization correlations from FIPPS is still in progress, we present in Fig. 5 the results of an analogous analysis for data obtained with the EXILL array, where eight Clover detectors were placed in a similar octagonal geometry. FIPPS provides a better energy resolution compared to EXILL setup, therefore for FIPPS, we expect similar results but with better precision.

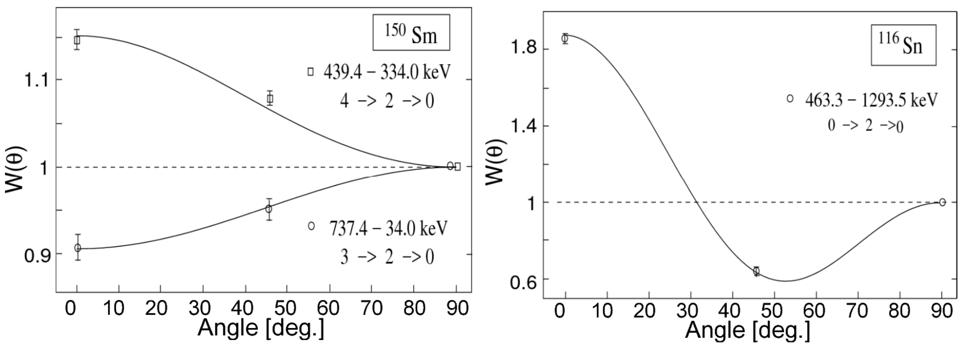

Fig. 5. Examples of angular correlations obtained for the EXILL setup for the 439.4–334.0 keV and 737.4–334.0 keV cascades in ^{150}Sm and the 463.3–1293.5 keV cascade in ^{116}Sn [14].

Angular correlations often give two possible solutions for the mixing ratio, δ of a γ-ray transition. Because in directional-polarization correlations there is an additional dependence on δ, a measurement of the linear polarization of the γ ray allows to find a unique solution, apart for the main result of such a measurement, which is the polarity of the transition, allowing to determine the parity of the initial level in the cascade.

The polarization-correlation theoretical values of linear polarization, $P_{\rm th}(\gamma)$, for a mixed dipole-plus-quadrupole transition can be calculated for the upper transition in a cascade from the formula

$$P_{\rm th}(\gamma_1) = \pm \frac{3A_2B_2 + \frac{5}{4}A_4B_4 + 4A_2(\gamma_2)\frac{2\delta_1 F_2(12I_0I_1)}{1+\delta_1{}^2}}{2 - A_2B_2 + \frac{3}{4}A_4B_4}\,. \tag{1}$$

In Eq. (1), the $+\,(-)$ sign applies to the M1+E2 (E1+M2) multipolarity of the studied γ-ray transition. Therefore, comparing the sign of the calculated and the experimental polarization, one can distinguish between the M1+E2 and E1+M2 multipolarities of this transition. The A_k, B_k and F_2, coefficients are given in Ref. [15].

The paramount condition for a successful measurement of linear polarization is the precise determination of the sensitivity calibration of the polarimeter instrument. For a clover-type Compton polarimeters, the Q_0 sensitivity is reduced by factor of 4 to 5 with respect to a point-like Compton polarimeter [16], due to the non-zero size of the scattering crystal and the close proximity of the absorbing crystal. In addition, there may be some extra dependence on the γ-ray energy, due to the finite size of the clover. The expected polarimeter sensitivity has then the form: $Q(E_\gamma) = Q_0(E_\gamma)[A + B \times E_\gamma]$.

In Fig. 6, we present newly obtained polarization sensitivity of the EXILL clover detectors determined experimentally in a wide energy range, from 200 keV to 8000 keV. The precision of the calibration ranges from about 5% at low E_γ to about 20% at $E_\gamma \approx 8000$ keV. For the FIPPS instrument, we expect a similar value of the sensitivity, however with smaller uncertainties of about 5% at $E_\gamma \approx 8000$ keV.

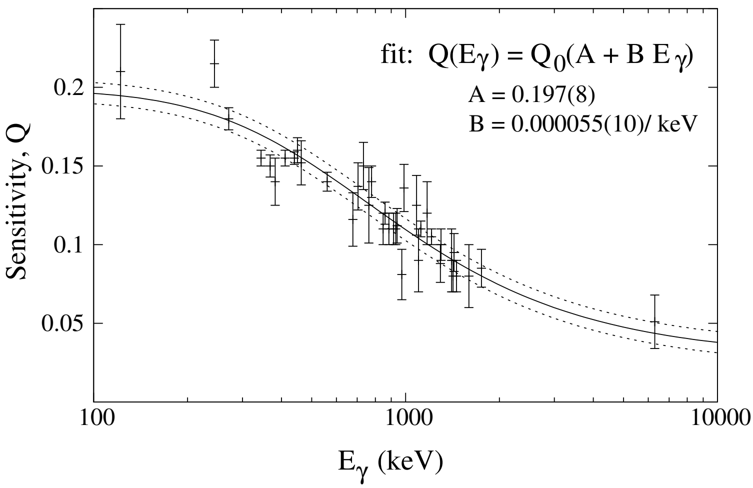

Fig. 6. Sensitivity Q of EXILL detectors for the polarization effect.

This work has been supported by the National Science Centre, Poland (NCN) under contract No. DEC-2013/09/B/ST2/03485.

REFERENCES

[1] W. Urban *et al.*, *Nucl. Phys. A* **689**, 605 (2001).
[2] W. Urban *et al.*, *Eur. Phys. J. A* **22**, 241 (2004).
[3] T. Togashi *et al.*, *Phys. Rev. Lett.* **117**, 172502 (2016).
[4] T. Rząca-Urban *et al.*, *Phys. Rev. C* **88**, 034302 (2013).
[5] M. Czerwiński *et al.*, *Phys. Rev. C* **88**, 044314 (2013).
[6] T. Materna *et al.*, *Phys. Rev. C* **92**, 034305 (2015).

[7] T. Rząca-Urban *et al.*, *Phys. Rev. C* **95**, 064302 (2017).

[8] W. Urban *et al.*, *Phys. Rev. C* **93**, 034326 (2016).

[9] H. Naïdia *et al.*, *Phys. Rev. C* **95**, 064303 (2017).

[10] A. Guessous *et al.*, *Phys. Rev. Lett.* **75**, 2280 (1995).

[11] W. Urban *et al.*, *Phys. Rev. C* **72**, 027302 (2005).

[12] J.A. Pinston *et al.*, *Phys. Rev. C* **74**, 064304 (2006).

[13] T. Thomas *et al.*, *Nucl. Phys. A* **947**, 203 (2016).

[14] W. Urban *et al.*, *JINST* **8**, P03014 (2013).

[15] K.S. Krane *et al.*, *Nucl. Data Tables* **11**, 351 (1973).

[16] W.D. Hamilton, ed., *The Electromagnetic Interaction in Nuclear Spectroscopy*, North-Holland Publishing, Amsterdam 1975.

[17] W. Urban *et al.*, *Phys. Rev. C* **94**, 044328 (2016).

[18] T. Aoki *et al.*, *At. Data Nucl. Data Tables* **23**, 349 (1979).